

Detailed Kinetics of Cyclopentadiene Decomposition Studied in a Shock Tube

ALEXANDER BURCAT, MICHAEL DVINYANINOV

Faculty of Aerospace Engineering, Technion—Israel Institute of Technology, Haifa 32000, Israel

Received 19 September 1995; revised 26 April 1996; accepted 17 October 1996

ABSTRACT: Mixtures of cyclopentadiene diluted with argon were used to investigate its decomposition pattern in a single pulse shock tube. The temperatures ranged from 1080 to 1550 K and pressures behind the shock were between 1.7–9.6 atm. The cyclopentadiene concentrations ranged from 0.5 to 2%. Gas-chromatographic analysis was used to determine the product distribution. The main products in order of abundance were acetylene, ethylene, methane, allene, propyne, butadiene, propylene, and benzene. The decomposition of cyclopentadiene was simulated with a kinetic scheme containing 44 species and 144 elementary reactions. This was later reduced to only 36 reactions. The ring opening process of the cyclopentadienyl radical was found to be the crucial step in the mechanism. © 1997 John Wiley and Sons, Inc. *Int J Chem Kinet* **29**: 505–514, 1997.

INTRODUCTION

Cyclopentadiene was proposed as an important intermediate in the process of simple aromatic hydrocarbon degradation.

The mechanism by which the cyclopentadienyl radical reacts has not been studied in detail. It is widely known that the decomposition of a fuel molecule is the first step in many oxidative reactions. Therefore decomposition studies were done in conjunction with the cyclopentadiene oxidation [1,2].

There are four studies of cyclopentadiene decomposition that we are aware of. Colket [1]

performed a shock tube study, and found for the reaction $c\text{-C}_5\text{H}_6 \rightleftharpoons \text{H} + c\text{-C}_5\text{H}_5$; $k = 2 \times 10^{15} \exp(-81000/RT) \text{ s}^{-1}$, for the temperature range 1100–2000 K and pressure range of 10–13 atm. Butler [2] and Bruisma et al. [3] performed experiments in a flow reactor. According to Butler [2], the cyclopentadienyl radical undergoes ring cleavage and there is a transition to straight chain aliphatic chemistry which is well understood. Butler [2] performed only a qualitative survey but Bruisma et al. [3] investigated the flame speed and product distribution. Gey et al. [4] published an ab-initio calculation with some limited qualitative experiments performed in a regular oven.

The formation of the cyclopentadienyl radical and its consumption involves a transition from cyclic to open chain kinetics. Thus understanding the role of the cyclopentadienyl radical, is crucial to linking these two chemical regimes which have been until now connected only by global mechanisms.

Correspondence to: A. Burcat

Contract grant Sponsor: G.I.F. German Israeli Foundation for Scientific Research and Development

Contract grant Sponsor: Ministry of absorption of Israel

Contract grant Sponsor: Technion Vice-President for Research fund

© 1997 John Wiley & Sons, Inc.

CCC 0538-8066/97/070505-10

Table I Mixtures of CPD and Argon used for Pyrolysis Experiments

Series	Symbol	[CPD] %	[Ar] %	p_1 ca. torr	P_5 atm.	No. of Runs
1	\triangle	1.01	98.99	75	1.8–3.0	58
2	\odot	0.50	99.50	75	1.7–2.5	45
3	∇	2.01	97.99	75	2.1–3.2	32
4	\square	0.70	99.30	225	5.6–9.6	27

EXPERIMENTAL

Apparatus

The pyrolysis was studied in a 54 mm i.d. pressurized driver, single pulse shock tube. This instrument serves as a heater in the millisecond range where the walls remain at room temperature. The shock tube is made of stainless steel, and is 4 m long. The driven section is 2.5 m long. Mylar diaphragms of different gauges were burst to generate the shock wave. The driver gas used was helium. Typical reaction times were 2 milliseconds. At the end of the reaction time an aerodynamic cooling of ca. 10^6 K/s is achieved.

The sampling section, 0.25 m long, contains three Kistler 603A piezo-electric transducers. Two transducers, 0.2 m apart, measure the shock velocity from

which the temperature is calculated. A third piezo-electric gauge, located on the end plate, records the pressure. The pressure-time output is fed to a Nicolet dual trace digital oscilloscope. Two 12 bit traces of 4098 points each, are recorded at 1 μ s intervals. One trace is connected to the end plate transducer and records the experimental dwell time, while the other is connected to the other two transducers in parallel and records the shock speed. The temperature uncertainty error is ± 20 K.

Analysis and Mixture Handling

Post-shock gas mixtures are extracted from the test section of the shock tube in preevacuated glass bulbs. The products of the reaction consist of the stable

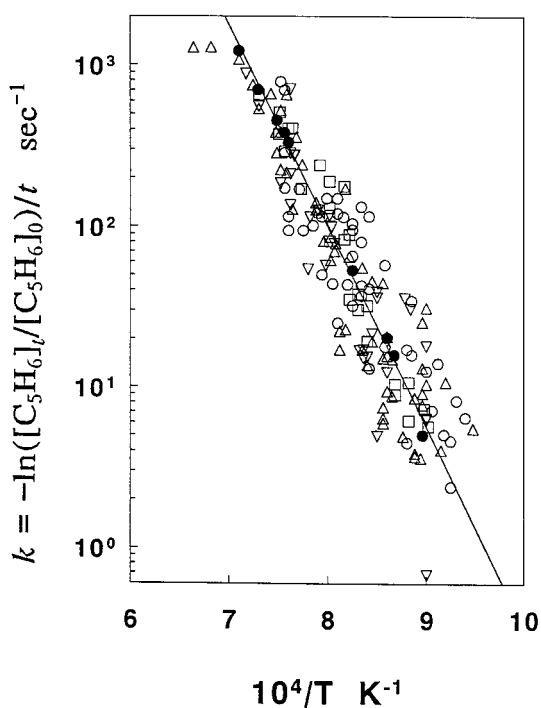


Figure 1 $\log k = -\ln([C_5H_6]_t/[C_5H_6]_0)/t$ vs. $10^4/T$ K, for the four mixtures appearing in Table I. The open symbols are the experiments. The closed symbols are the simulation values for the same mixtures. The calculations with the reduced mechanism, coincide with full mechanism. The activation energies obtained for the experimental and simulated points were 50 and 57.0 kcal/mole.

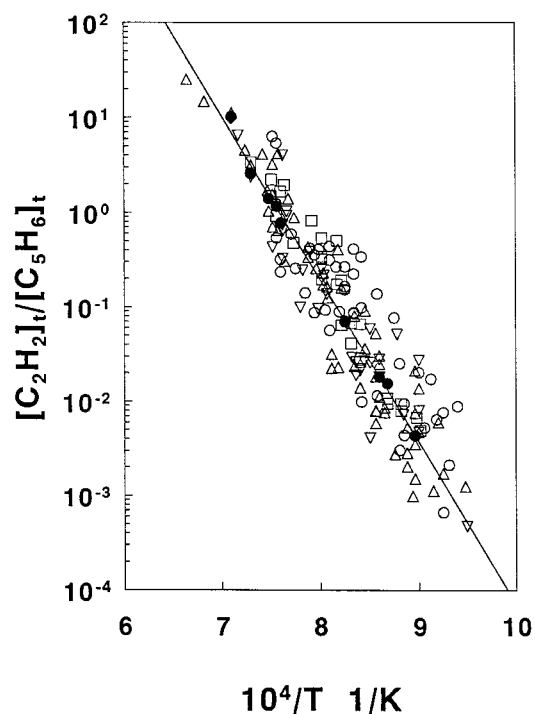


Figure 2 Results of gas chromatographic analysis for acetylene on a logarithmic scale of $([C_2H_2]_t/[C_5H_6]_t)$ vs. $10^4/T$ K for the four mixtures in Table I. The black symbols represent the simulated values obtained for the same mixture. The activation energy obtained was 74 and 79 kcal/mole for the experimental and simulated points, respectively.

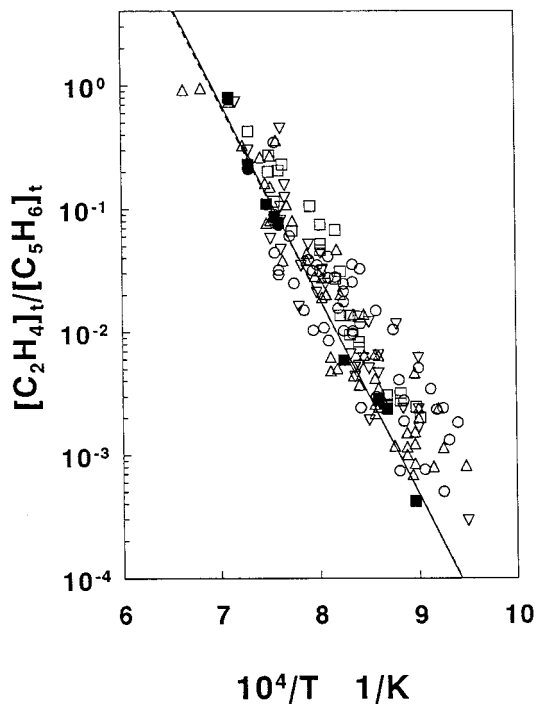


Figure 3 Results of gas chromatographic analysis for ethylene on a logarithmic scale of $([C_2H_4]_t/[C_5H_6]_t)$ vs. $10^4/T$ K for the four mixtures in Table I. The black squares represent the simulated values obtained for the same mixture. The activation energy was 58. and 73. kcal/mole for the experimental and simulated points, respectively.

species found after the aerodynamic cooling. The reacted gas is injected into a HP 8900 series gas-chromatograph equipped with a flame ionization detector and containing a 6 feet long Porapak N column.

The output of the ionization detector is transferred to a Perkin-Elmer/Nelson Analytical PC Integrator. The unit, performs on-line area calculations in comparison with standard samples.

Cyclopentadiene (CPD) tends to dimerise $[(C_5H_6)_2]$. The di-cyclo-pentadiene used was Riedel-Haën AG listed as 95% pure. To obtain the monomer, the dimer was heated in a flask under constant pumping to get rid of lighter weight impurities, and the vapors were distilled through a preheated oven at 483°C directly into a preevacuated stainless steel cylinder. The cylinder was then pressurized with argon to 50 psia using Herzliya 99% pure argon. To ensure thorough mixing of the gases, the mixtures were left for 48 h before use. The concentration of CPD in the cylinders did not change during a period of 6 weeks. Gas chromatographic analyses showed that the fuel in the mixture consisted of more than 99% C_5H_6 , ca. 0.2–0.4% CH_4 (originating in the argon), less than 0.1% butadiene and less than 0.1% of an unknown higher weight compound, probably a C_6 .

Calculations

The reflected shock temperatures were calculated using standard conservation equations and the ideal gas equation of state, assuming frozen chemistry. Thermodynamic data for all the species were taken from a recent compilation [5].

RESULTS

162 runs were performed with mixtures of cyclopentadiene diluted in argon. The 4 different mixtures are listed in Table I.

The first-order rate constant of the overall decomposition of CPD is shown in Figure 1 as $\log k$ vs. $1/T$. k is given by:

$$k = \frac{-\ln([C_5H_6]_t/[C_5H_6]_0)}{t} \text{ s}^{-1}.$$

Figures 2–9 show the concentrations of the products relative to the final concentrations of cyclopentadiene plotted on a logarithmic scale vs. $1/T$.

$\log([product]_t/[C_5H_6]_t)$ vs. $1/T$.

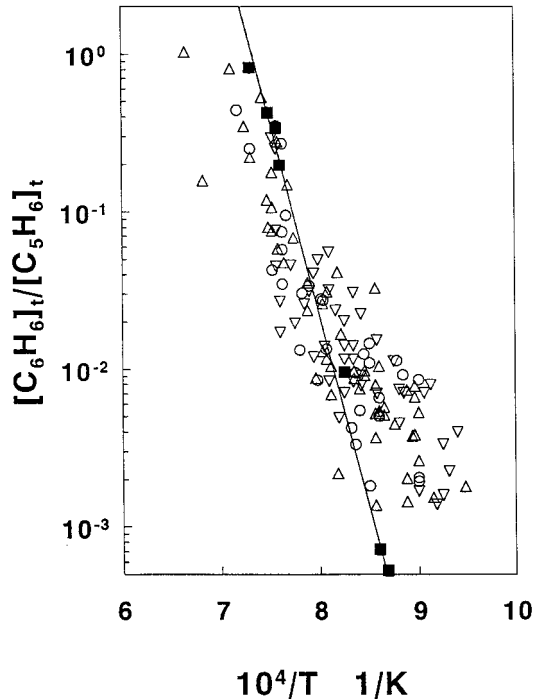


Figure 4 Results of gas chromatographic analysis for benzene on a logarithmic scale of $([C_6H_6]_t/[C_5H_6]_t)$ vs. $10^4/T$ K for the four mixtures in Table I. The black squares represent the simulated values obtained for the same mixture. The activation energy was 50. and 110. kcal/mole for the experimental and simulated points, respectively.

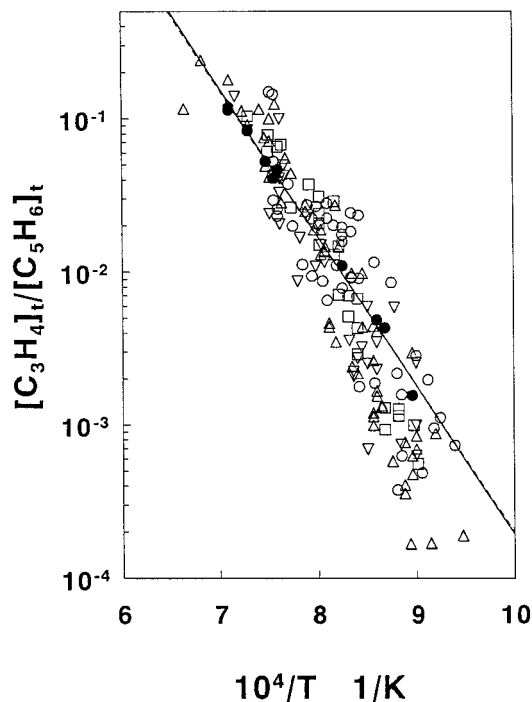


Figure 5 Results of gas chromatographic analysis for allene on a logarithmic scale of $[C_3H_4]_t/[C_5H_6]_t$ vs. $10^4/T$ K for the four mixtures in Table I. The black symbols represent the simulated values obtained for the same mixture. The activation energy was 56.0 and 45. kcal/mole for the experimental and simulated points, respectively.

Results are shown for acetylene, ethylene, benzene, allene, propyne, propylene, methane, and 1,3-butadiene. An additional unidentified C_4 specie was also recorded in quantities similar to butadiene. The data from the four mixtures (Table I) are drawn with the symbols shown in the table. The filled symbols represent kinetic calculations performed for mixtures of the same composition and pressure. These computations are discussed further on.

The H/C ratio of CPD is 1.2 while the products reported except C_2H_2 and C_6H_6 have a higher ratio. In order to verify the H/C ratio balance all the concentrations of the products except CPD were summed up according to the carbon content and again according to the hydrogen content. Thus C_2H_4 was considered first as $2/5 [C_2H_4]$ for the carbon sum and $4/6 [C_2H_4]$ for the hydrogen content. This was repeated for all the products. Summing up all products except CPD we got the sum of $[C]/6$ and the sum of $[H]/6$ for each experiment. These were plotted in Figure 10 one against the other on a logarithmic scale. A perfect result would be a 45 degree line, and our result is approximately correct with a 10–15% carbon deficiency at low temperatures. The reason for this may be inaccuracies in the gas chromatographic calibration.

The total carbon balance (including CPD) is 90–95% up to 1240 K, then it drops to 85% at 1300 K and from there it drops rapidly to 60% at 1370 K. At these temperatures soot is formed, but was not analyzed quantitatively.

COMPUTATIONS

Simulation of cyclopentadiene decomposition was performed with the CHEMKIN [6] kinetic program. The program input included forward reaction rates and thermodynamic polynomials for all the participating species in addition to temperature, pressure, and concentrations of the reactants. The program calculates rate constant of the back reaction for every reaction given, through the equilibrium constant using the thermodynamic functions of the species involved. The computed time is equal to the experimental constant temperature dwell time. No calculations during the cooling period were performed.

A kinetic scheme containing 144 reactions was proposed. The reactions were gathered from well established kinetic schemes. Those reaction rates have

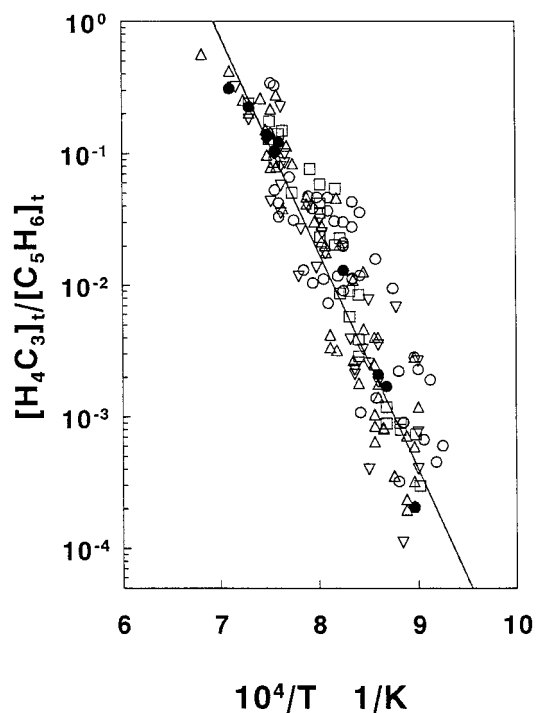


Figure 6 Results of gas chromatographic analysis for propyne on a logarithmic scale of $[H_4C_3]_t/[C_5H_6]_t$ vs. $10^4/T$ K for the four mixtures in Table I. The black symbols represent the simulated values obtained for the same mixture. The activation energy obtained was 70 and 75 kcal/mole for the experimental and simulated points, respectively.

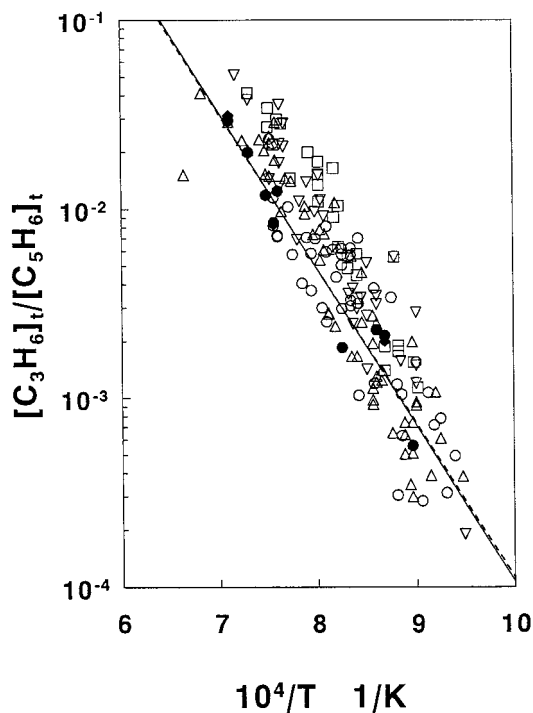


Figure 7 Results of gas-chromatographic analysis for propylene on a logarithmic scale of $([C_3H_6]_t/[C_5H_6]_t)$ vs. $10^4/T$ K for the four mixtures in Table I. The black symbols represent the simulated values obtained for the same mixture. The activation energy obtained was 41.0 and 38. kcal/mole for the experimental and simulated points, respectively.

been verified by many kineticists, so their values are well accepted [7,8,8(a)]. Additionally, specific reactions were added from other sources. The first 37 reactions were taken from the scheme for methane oxidation GRI-Mech developed for C_1 — C_2 species [7]. 14 reactions were taken from a study by Butler [9]. The C_3 — C_4 model containing 54 reactions was added to this scheme from Westbrook et al. [8,8(a)]. Westbrook does not identify between allene and propyne. In this study this species was considered to be propyne ($CH_3-C\equiv CH$) and was identified in the computer scheme as H_4C_3 . In addition 9 reactions were added from Miller and Melius [10], and two reactions were taken from Frenklach et al. [11]. Finally, 10 reactions were taken from Dean [12], 3 reactions were taken from Kern et al. [13,14], and one reaction from Tsang and Hampton [15] and Warnatz [16]. The thermodynamic data for the CHEMKIN program were taken from a recent compilation [5] and the cyclopentadiene and derived radicals were taken from a recent study [17].

A sensitivity analysis was performed in which the scheme was tested by the elimination of each of the reactions consecutively. The final concentration of

the cyclopentadiene at time t after the elimination of a reaction was compared to the final concentration of cyclopentadiene in the standard 144 step scheme. The most sensitive reactions were gathered to a reduced scheme. This reduction method was defined by Frenklach as “brut-force third degree reduced scheme” [18]. The reduced scheme included 36 reactions only, and showed results identical with the full scheme. All the species recorded experimentally could be reproduced with the reduced mechanism.

The sensitivity analysis was performed for total cyclopentadiene decomposition and the individual products acetylene, ethylene, benzene, allene, propyne, propylene, and butadiene, and the results are summarized in Tables II and III.

DISCUSSION

The modeling of a scheme containing 144 reactions creates a problem of understanding the details in such a large mechanism. The elimination of relatively unimportant reactions is therefore essential.

The reduced mechanism of 36 reactions is shown

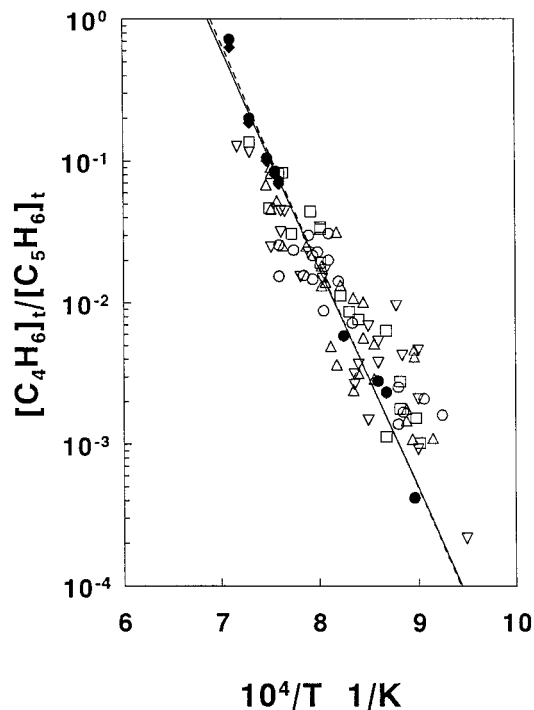


Figure 8 Results of gas chromatographic analysis for 1,3-butadiene on a logarithmic scale of $([C_4H_6]_t/[C_5H_6]_t)$ vs. $10^4/T$ K for the four mixtures in Table I. The black symbols represent the simulated values obtained for the same mixture. The black rhombuses represent the values obtained for the reduced mechanism. The activation energy obtained was 47 and 69 kcal/mole for the experimental and simulated points, respectively.

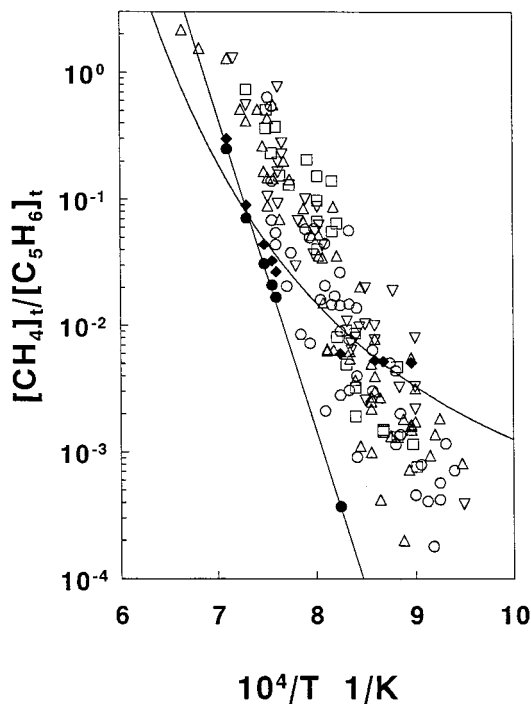


Figure 9 Results of gas-chromatographic analysis for methane on a logarithmic scale of $([CH_4]_t/[C_5H_6]_t)$ vs. $10^4/T$ K for the four mixtures in Table I. The black symbols represent the simulated values obtained for the same mixture. The black rhombuses represent the values obtained for a mechanism containing 0.5% of the total fuel. The activation energy obtained was 70 and 113 kcal/mole for the experimental and simulated points, respectively.

in Table IV. The results of the computer modeling using the full and reduced mechanism are shown in Figures 1–9 by filled symbols where the main decomposition products are modeled. The results of the full scheme are shown with filled circles and those of the reduced mechanism with filled rhombuses. In most cases both symbols fall one on the top of the other.

It can be seen that in Figures 1–9 the agreement between the experiment and computation is very good with the exception of methane. Our experiments show excessive methane over the predicted mechanism. In Figure 9 the presence of 0.5% CH_4 of the fuel concentration is plotted using black rhombuses. It points out that this may be the cause of the existing discrepancy.

In Table V a list of the experimental activation energies for the different products is compared with the activation energy of the calculated points as they appear in Figures 1–9. The comparison is relatively good to excellent except for benzene and methane.

A list of the most sensitive reactions in the decomposition scheme of cyclopentadiene is shown in

Table II and for the production of acetylene, ethylene, benzene, allene, propyne, propylene, and butadiene at the low and high temperature range are listed in Table III.

The numbers appearing in the third and fifth column of Table II are the ratio of the decomposition of cyclopentadiene in the absence $[C]_{det}$ and the presence $[C]_{stan}$ of the respective reaction of the 144 step mechanism source. The numbers appearing in the third and fifth column of Table III are the ratio of the concentration at time t of the species in the absence $[C]_{det}$ and the presence $[C]_{stan}$ of the respective reaction in the standard 144 step mechanism source.

As expected the first reactions are the decomposition of cyclopentadiene, either by spontaneous loss of a hydrogen atom or by a hydrogen atom attack



The sensitivity analysis confirms that these two reactions are the most sensitive and the fifth most sensitive reaction at the low temperature end (1116 K), and as number one and four, respectively, at the high temperature end (1409 K), when the cyclopentadiene decomposition is tested. The 0 number for Reaction (1) means that the scheme cannot be calculated without this reaction. The rate constant for reaction (1) that fits best our study is $k = 5 \times 10^{15} \exp(-78682/RT) s^{-1}$. But in the case of the oxidation of cyclopentadiene [19] this value fits well the low temperature end while at the higher temperature end, around 2000 K, Dean's [12] value $k =$

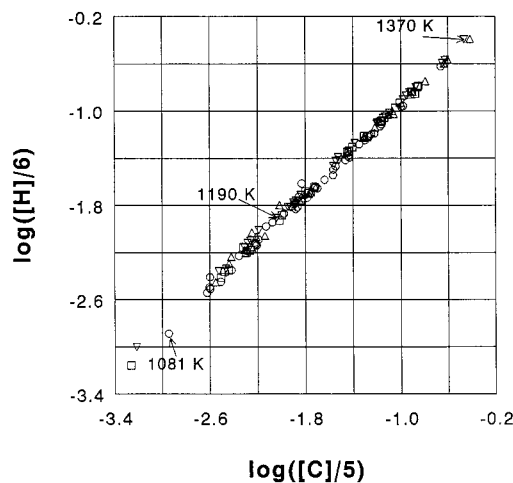


Figure 10 The sum of $[H]/6$ vs. the sum of $[C]/5$ for all the products except CPD in the four different mixtures from Table I. A perfect agreement should be a 45° line.

Table IV Reduced Kinetic Scheme for the Decomposition of Cyclopentadiene

Reaction	$\Delta_r H$	A	n	E	Ref.
	(1200 K) kcal/mole				
1. $C_5H_6 \rightleftharpoons C_5H_5 + H$	86.3	5.00E + 15	0	78682	This work
2. $C_5H_6 + H \rightleftharpoons C_5H_5 + H_2$	-20.30	4.00E + 13	0	3000	[12]
3. $C_5H_5 \rightleftharpoons H_5C_5^\psi$	33.3	5.00E + 13	0	33300	This work
4. $C_5H_2 + C_3H_3 \rightleftharpoons H_5C_5^\psi$	-40.4	5.00E + 12	0	0	This work
5. $C_3H_3 + C_3H_3 \rightleftharpoons C_6H_5 + H$	-34.5	2.00E + 12	0	3000	This work
6. $C_5H_6 + C_2H_3 \rightleftharpoons C_5H_5 + C_2H_4$	-27.54	6.00E + 12	0	0	[9]
7. $C_5H_6 + C_3H_3 \rightleftharpoons C_5H_5 + C_3H_4$	-5.2	1.10E + 11	0	5500	This work
8. $C_5H_6 + C_3H_5 \rightleftharpoons C_5H_5 + C_3H_6$	-4.2	1.10E + 11	0	5500	This work
9. $C_5H_6 + C_6H_5 \rightleftharpoons C_5H_5 + C_6H_6$	-26.2	3.10E + 11	0	5500	This work
10. $C_5H_6 + CH_3 \rightleftharpoons C_5H_5 + CH_4$	-21.46	3.11E + 11	0	5500	[12]
11. $C_3H_5 + C_3H_5 \rightleftharpoons C_5H_6 + C_3H_4$	-27.07	1.00E + 13	0	0	[12]
12. $C_3H_5 + C_3H_5 \rightleftharpoons C_6H_{10}$	-66.6	5.00E + 13	0	0	This work
13. $C_6H_{10} \rightleftharpoons C_4H_6 + C_2H_4$	24.17	1.00E + 12	0	24000	This work
14. $C_2H_2 + CH_3 \rightleftharpoons C_3H_5$	-48.88	1.10E + 45	-9.4	35410	[12]
15. $C_3H_5 + C_3H_5 \rightleftharpoons C_3H_6 + C_3H_4$	-30.93	1.00E + 12	0	0	[12]
16. $H + C_2H_2 (+M) \rightleftharpoons C_2H_3 (+M)$	-43.06	5.60E + 12	0	2400	[7]
17. $H_7C_5^\psi \rightleftharpoons C_5H_6 + H$	45.92	1.02E + 58	-13.1	60160	[12]
18. $C_3H_5 + C_2H_2 \rightleftharpoons C_5H_6 + H$	-86.46	2.95E + 32	-5.8	25730	[12]
19. $H_7C_5^\psi \rightleftharpoons C_5H_7^\psi$	14.96	1.52E + 58	-13.1	60600	[12]
20. $C_3H_5 + C_2H_2 \rightleftharpoons H_7C_5^\psi$	-55.09	3.42E + 52	-12.2	27980	[12]
21. $C_3H_5 + C_2H_2 \rightleftharpoons C_5H_7^\psi$	-40.05	8.38E + 30	-6.2	12820	[12]
22. $C_2H_2 + C_2H_2 \rightleftharpoons C_4H_3 + H$	60.3	1.00E + 13	0	45000	[8(a)]
23. $C_3H_6 + H \rightleftharpoons C_3H_5 + H_2$	-16.48	5.01E + 12	0	1500	[8(a)]
24. $C_3H_6 \rightleftharpoons C_3H_5 + H$	90.37	5.90E + 47	-9.48	107300	[12]
25. $H + CH_4 \rightleftharpoons CH_3 + H_2$	1.3	6.60E + 08	1.6	10840	[7]
26. $H_4C_3^\psi + H \rightleftharpoons C_3H_3 + H_2$	-12.65	5.00E + 08	2	5000	[10]
27. $C_4H_3 + C_2H_2 \rightleftharpoons C_6H_5$	-92.98	2.80E + 03	2.9	1400	[10]
28. $C_3H_4 \rightleftharpoons H_4C_3^\psi$	-1.5	2.00E + 14	0	62000	[22]
29. $C_3H_4 + H \rightleftharpoons C_3H_3 + H_2$	-15.18	5.00E + 08	2	5000	[10]
30. $H_4C_3^\psi \rightleftharpoons C_3H_3 + H$	92.95	8.88E + 29	-4.41	98200	[12]
31. $C_3H_7 \rightleftharpoons CH_3 + C_2H_4$	23.02	3.00E + 14	0	32960	[16]
32. $C_3H_7 \rightleftharpoons H + C_3H_6$	34.65	1.25E + 14	0	37000	[16]
33. $C_6H_6 + H \rightleftharpoons C_6H_5 + H_2$	8.86	3.00E + 07	2	5000	[10]
34. $C_6H_5 + H \rightleftharpoons C_6H_6$	-115.3	5.00E + 13	0	0	[10]
35. $H + C_2H_4 \rightleftharpoons C_2H_3 + H_2$	7.24	1.32E + 06	2.53	12240	[15]
36. $C_4H_6 \rightleftharpoons 2CH_3$	104.4	3.98E + 19	-1	98150	[8(a)]

ψ —The species H_5C_5 represents the radical 3pentene-lyne-5yl. H_4C_3 represents propyne. H_7C_5 is the cyclopentene radical and C_5H_7 is the linear 1,3-pentadien-5yl radical. C_4H_6 is 1,3 butadiene.

$8.13 \times 10^{24} T^{-2.981} \exp(-78682/RT) s^{-1}$ fits better with very little influence on our computations.

Three cyclopentadienyl radicals can be formed: 2,4-cyclopentadiene-1yl, 1,3-cyclopentadiene-1yl, and 1,3-cyclopentadiene-2yl. The first is the only one electronically stabilized. Despite the stabilization the double bonds are definitely shorter than the single bonds as shown by calculations [17,20]. Thus its symmetry is C_{2v} ($\sigma = 2$) and not D_{5h} ($\sigma = 10$). This radical is easier to obtain since the H—C bond on a double bond carbon is stronger than on a primary carbon. Therefore only the first possibility was taken into account [20].

The cyclopentadienyl radical undergoes a ring opening process, and this reaction is a key reaction in the proposed mechanism. Without this value an agreement between the calculated and the experimental results cannot be achieved.



This reaction is the second most important reaction at the low temperature end, and at high temperatures.

In the ring opening of cyclopentadiene, since the conjugated C—C bond is unlikely to break, the most probable linear species is 3-pentene-1yne-5yl

Table V A Comparison of Experimental and Calculated Results

Species	Experimental Activation Energy kcal/mole	Calculated Activation Energy kcal/mole	Figure
Cyclopentadiene	50	57	1
Acetylene	74	79	2
Ethylene	58	73	3
Benzene	50	110	4
Allene	56	45	5
Propyne	70	75	6
Propylene	41	38	7
1,3-Butadiene	47	69	8
Methane	70	113	9

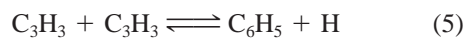
$\text{HC}\equiv\text{C}-\text{CH}=\text{CH}-\text{CH}_2\cdot$ although a hydrogen atom must perform a two carbon displacement (see Fig. 11). The thermochemistry of this linear radical was estimated [5] with the help of the NIST 1994 Structures and Properties program [21]. The heat of formation of the linear radical was approximated as $\Delta_f H_{298} = 97.1 \pm 2.0$ kcal.

The linear C_5H_5 radical can break into acetylene and propargyl radical (in this scheme by the reverse reaction):



This reaction is the third most important reaction at the low temperature end as well as at the high temperature end. It is the third most important for the formation of acetylene and propylene, low temperature propyne, and high temperature ethylene and butadiene, as well as number 4 for low temperature allene and high temperature benzene.

The propargyl radical is a precursor for the production of benzene or phenyl radicals:



This reaction plays an important role at high temperatures but not at low temperatures except for benzene. This reaction reported by Miller and Melius [10] had to be slightly changed to fit our experimental values. We reduced its preexponential factor and slightly increased its activation energy.

The reactions of cyclopentadiene with vinyl, propargyl, allyl, phenyl, and methyl radicals are the next important steps. Specifically reaction (7) which is the fourth in importance for the CPD decomposition acetylene and propyne formation, second for allene formation, etc. but only at low temperatures.



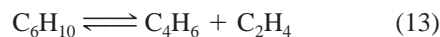
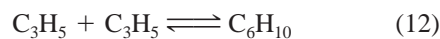
Reaction (8) follows it in some cases



The reaction of the cyclopentadienyl radical with C_3H_5 to form cyclopentadiene and allene is also of high importance.



Reactions 12 and 13 are important at low as well as at high temperatures for the formation of ethylene, allene, propyne, and propylene.



Finally the isomerisation of allene \leftrightarrow propyne is very

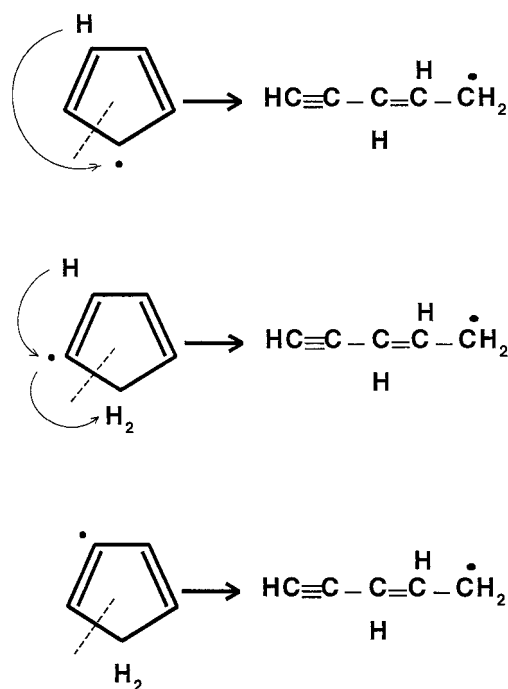


Figure 11 The three possible cyclopentadienyl radicals and the ring opening path.

important, and the rate constant of this reaction that fits best is the one found experimentally [22].



In conclusion, the reduced mechanism permits the decipheration of the decomposition mechanism, and points out the most important reaction in the process which is the ring opening. It also reproduces almost exactly the results obtained with the full mechanism. The full mechanism, however, can reproduce the production of additional species, many of which were not identified in this study but were reported in experiments using mixtures with higher concentration of cyclopentadiene [2].

This research was supported by a grant from the G.I.F. German Israeli Foundation for Scientific Research and Development. M. D. also acknowledges partial funding by a grant from the Ministry of absorption of Israel, and by a grant from the Technion Vice-President for Research fund. The authors thank Dr. E. Olchansky and Dr. C. Sokolinsky for computer simulation. Special thanks are extended to Prof. Assa Lifshitz for very fruitful discussions.

BIBLIOGRAPHY

1. M. B. Colket, *The Pyrolysis of Cyclopentadiene*, Eastern States Section of Combustion Institute annual meeting, Orlando, 1990, Paper 1.
2. R. G. Butler, *A Flow Reactor Study of the Oxidation of 1,3-Cyclo-Pentadiene*, MSc. Thesis, Princeton University, 1992.
3. O. S. L. Bruisma, P. J. J. Tromp, H. J. J. de Sauvage Nolting, and J. A. Moulijn, *Fuel*, **67**, 334 (1988).
4. E. Gey, B. Ondrushka, and G. Zimmermann, *J. Prakt. Chem.*, **329(3)**, 511 (1987).
5. A. Burcat and B. McBride, *1995 Thermodynamic Database for Combustion and Air Pollution Use*, Technion Aerospace Engineering (TAE) Report # 732, January 1995.
6. J. Kee, F. M. Rupley, and J. A. Miller, *Chemkin-II A Fortran Chemical Kinetic Package for Analysis of Gas Phase Chemical Kinetics*. Sandia Report SAND 89-8009B. U.C-706, 1992.
7. R. V. Serkauskas, M. Frenklach, H. Wang, C. T. Bowman, G. P. Smith, D. M. Golden, W. C. Gardiner, and V. Lissianski, *An Optimized Detailed Chemical Mechanism for Methane Combustion*, Gas Research Institute Topical Report 1994.
8. C. K. Westbrook, W. J. Pitz, M. M. Thornton, and P. C. Malte, *Comb. Flame*, **72**, 45 (1988); W. J. Pitz, C. K. Westbrook, W. M. Proscia, and F. L. Dryer, *A Comprehensive Chemical Kinetic Reaction Mechanism for the Oxidation of N Butane*, *20-th Comb. Symp.*, 1984, pp. 831–843.
9. J. L. Emdee, K. Brezinsky, and I. Glassman, *J. Phys. Chem.*, **96**, 2151, (1992), F. N. Egolffopoulos, D. X. Du, and C. K. Law, *Comb. Sci. Tech.*, **83**, 33 (1992).
10. J. A. Miller and C. F. Melius, *Combust. Flame*, **91**, 21 (1992).
11. M. Frenklach, D. W. Clary, T. Yuan, W. C. Gardiner, and S. E. Stein, *Combust. Sci. Technol.*, **50**, 79 (1986).
12. A.M. Dean, *J. Phys. Chem.*, **94**, 1432 (1990).
13. R. D. Kern, K. Xie, H. Chen, and J. H. Kiefer, *High Temperature Pyrolysis of Acetylene and Diacetylene behind Reflected Shock Waves*, *23 Combust Symp.*, (1990), pp. 69–75.
14. C. H. Wu, and R. D. Kern, *J. Phys. Chem.*, **91**, 6291 (1987).
15. W. Tsang and R. F. Hampson, *J. Phys. Chem. Ref. Data*, **15**, 1087 (1986).
16. J. Warnatz, *Chemistry of High Temperature Combustion of Alkanes up to Octane*, *20-th Comb. Symp.*, 1984, pp. 845–855.
17. M. Karni, I. Oref, and A. Burcat, *J. Phys. Chem. Ref. Data*, **20**, 665 (1991).
18. M. Frenklach, *Reduction of Chemical Reaction Models in Numerical Approaches to Combustion Modeling*, Chap. 5, E. S. Oran and J. P. Boris, Eds., *Progress in Astronautics & Aeronautics*, 1991, Vol. 135, pp. 129–154.
19. A. Burcat, M. Dvinyaninov, E. Olchanski, and Ch. Sokolinski, *Detailed Combustion Kinetics of Cyclopentadiene*, *Combust. Flame*, submitted.
20. C. F. Melius, BAC/MP4 ab-initio calculation database, Sandia Co.
21. S. E. Stein, *NIST Structures and Properties*, Computerized Database #25, Gaithersburg, Maryland, 1994.
22. A. Lifshitz, M. Frenklach, and A. Burcat, *J. Phys. Chem.*, **79**, 1148 (1975).